Vital role for *Plasmodium berghei* Kinesin8B in axoneme assembly during male gamete formation and mosquito transmission

D. Depoix[1*], S.R. Marques[2], D.J.P. Ferguson[3], S. Chaouch[1], T. Duguet[1,4], R.E. Sinden[2], P. Grellier[1], L. Kohl[1]

[1] UMR 7245 CNRS Molécules de Communication et Adaptation des Micro-organismes, Muséum National d'Histoire Naturelle, Sorbonne Universités, CP52, 61 rue Buffon, 75231 Paris Cedex 05, France

[2] Department of Life Sciences, Imperial College of London, London, United Kingdom

[3] Nuffield Department of Clinical Laboratory Science, University of Oxford, Oxford, United Kingdom

[4] Institute of Parasitology, Macdonald Campus, McGill University 21, 111 Lakeshore Road H9X3V9, Sainte-Anne-de-Bellevue QC, Canada

Running title: *PbKIN8B* is crucial for male gametogenesis and life cycle

Corresponding author:

Delphine Depoix, delphine.depoix@mnhn.fr

Summary

Sexual development is an essential phase in the *Plasmodium* life cycle, where male gametogenesis is an original and extraordinarily rapid process. It produces 8 haploid motile microgametes, from a microgametocyte within 15 minutes. Its unique achievement lies in linking the assembly of 8 axonemes in the cytoplasm to the three rounds of intranuclear genome replication, forming motile microgametes, which are in a process called exflagellation. Surprisingly little is known about the actors involved in this process. We were interested in kinesins, molecular motors that could play potential roles in male gametogenesis. We have undertaken a functional characterization in *Plasmodium berghei* of a kinesin identified in male gametocytes and gametes, kinesin-8B (PbKIN8B). By generating *Pbkin8B-gfp* parasites, we show that PbKIN8B is specifically expressed during male gametogenesis and is associated with the axoneme. We created a *ΔPbkin8B* knockout cell line and analysed the consequences of absence of PbKIN8B on male gametogenesis. In *ΔPbkin8B* knockout cells, microtubule based motility is not affected in asexual mitoses and motility in the merozoite/ookinete similar to wild type cells. We show that the ability to produce sexually differentiated gametocytes is not affected in *ΔPbkin8B* parasites and that the 3 rounds of genome replication occurred normally. Nevertheless, the development to free motile microgametes was halted and the life cycle was interrupted *in vivo*. Ultrastructural analysis revealed that intranuclear mitoses were unaffected whereas cytoplasmic microtubules although assembled in doublets and elongated, failed to assemble in the normal axonemal “9+2” structure and become motile. Absence of a functional axoneme prevented microgamete assembly and release from the microgametocyte, severely reducing infection of the mosquito vector. This is the first functional study of a kinesin involved in male gametogenesis. Taken together, these results confirm a previously unknown role for PbKIN8B in male gametogenesis, providing new insights into *Plasmodium* flagellar organization.

Introduction

Plasmodium parasites infect a large number of animal species and are responsible for malaria in humans. In 2017, an estimated 219 million cases of malaria and 435 000 malaria deaths were reported worldwide (WHO report 2018). In most cases, malaria infections in humans are treated by artemisinin-based combination therapies, where 2 effective components with different modes of action and pharmacokinetic properties are combined. Emerging drug resistance makes it essential to search for new anti-malaria compounds and new targets in the parasite (Ouji, Augereau, Paloque, & Benoit-Vical, 2018) as no efficient vaccine for malaria is currently available.

During its life cycle, *Plasmodium* alternates between a vertebrate host and an insect vector, the female *Anopheles* mosquito. With an infective bite, the mosquito injects sporozoites in the vertebrate host, where they invade and multiply asexually, first in liver cells, and then in red blood cells. During the erythrocytic phase, a small fraction of parasites differentiate into sexual stages, male and female gametocytes. Circulating gametocytes are arrested at a G_0-like stage until they are taken up by a mosquito. In the mosquito midgut, gametocytogenesis is activated when parasites are exposed to a drop in temperature, a pH increase and to xanthurenic acid (XA) (Billker et al., 1998; Sinden, 1983; Sinden, Canning, & Spain, 1976). These changes trigger Ca^{2+} mobilization from internal stores which requires active cGMP-dependent protein kinase G (Bennink, Kiesow, & Pradel, 2016; Billker et al., 2004). While female gametogenesis requires limited morphological changes beyond escape from the host erythrocyte, male gametogenesis involves rapid and spectacular changes (Sinden et al., 1976). In the first few minutes after activation, male gametocytes egress from the red blood cells and three rounds of rapid intranuclear DNA replication take place, resulting in a uninucleate cell with a DNA content of 8C. This is accompanied by, and physically linked to, the simultaneous formation of 8 axonemes in the cytoplasm. *Plasmodium* axonemes display a classical “9+2” structure: 9 doublets of microtubules arranged in a circular pattern surrounding a central pair of singlet microtubules (reviewed in (Ishikawa, 2017)). Their mode of assembly is unusual: *Plasmodium* axonemes are assembled in the cytoplasm of the microgametocyte independent of Intraflagellar Transport, a

bidirectional transport machinery essential for the construction of flagella in most other eukaryotes (Prevo, Scholey, & Peterman, 2017). The components of the axoneme, such as tubulin, are ubiquitous in the cytoplasm and are assembled upon activation. The nuclear envelope does not break down during the 3 mitotic replications. The axonemes are however linked to the genome though spindle poles situated in nuclear pores to the 8 replicated haploid genomes in the nucleus, thus forming 8 flagellated motile microgametes, which, following violent axonemal 'swimming' are expelled from the microgametocyte in an exceptionally fast process called "exflagellation" (Sinden, 1983; Sinden et al., 1976). The motile gametes swim towards the female gametes to achieve fertilization, resulting in a zygote. The zygote develops into a motile and invasive ookinete, which after attachment and migration through the midgut epithelium, transforms into an oocyst. After approximately two weeks, the oocyst gives rise to sporozoites which migrate to the salivary glands and continue the parasite life cycle when injected into a new host (Bennink et al., 2016).

The sexual phase is essential to the parasite life cycle and considerable progress has been made in recent years in elucidating the molecular mechanisms governing this important differentiation process. In particular, a number of critical transcription factors and epigenetic regulators have emerged as crucial elements in the regulation of *Plasmodium* sexual commitment. The identification of these factors allowed a better understanding of the events occurring prior to and during commitment to sexual development (Filarsky et al., 2018; Kafsack et al., 2014; Kent et al., 2018; Sinha et al., 2014). However, surprisingly little is known about the dramatic processes and the actors leading to a free motile male gamete e.g. the molecular foundation of microgametes and how they are expelled from the microgametocyte. These dynamic processes will certainly require motor proteins, such as kinesins and dyneins, to transport cargoes, assemble the structure and generate the force for motility. Most dyneins, involved in motility, are part of the complex organisation of outer and inner dynein arms present on each doublet microtubule (Oda, Abe, Yanagisawa, & Kikkawa, 2016; Roberts, Kon, Knight, Sutoh, & Burgess, 2013). The only information on dynein arm structure in *Plasmodium* available at the moment is that it is different from other organisms (Francia, Dubremetz,

& Morrissette, 2015). We therefore selected to study the roles of kinesins, in particular their role in microgametogenesis.

Only 10 kinesin encoding genes are found in the *P. berghei* genome, fewer than in other eukaryotes (Wickstead, Gull, & Richards, 2010). Their expression varies during the parasite life cycle. Three kinesins have been identified in proteomic studies of male gametogenesis (C. H. S. Garcia et al., 2018; Khan et al., 2005; Talman et al., 2014). According to the comprehensive study of kinesins across eukaryotes by Wickstead et al. (2010), they belong to the families kinesin-8B, -13 and -15. We chose to examine the role of kinesin-8B, referred to as PbKIN8B in the rest of the manuscript.

While most kinesins display predominantly one activity, either transport along microtubules or depolymerization, kinesin-8 family members are reported multitalented. They can walk on microtubules, but they also regulate microtubule length, during mitosis (Gergely, Crapo, Hough, McIntosh, & Betterton, 2016; Grissom et al., 2009; Gupta, Carvalho, Roof, & Pellman, 2006; McHugh, Gluszek, & Welburn, 2018; Savoian & Glover, 2010), and/or ciliary and flagellar assembly (Hu, Liang, Meng, Wang, & Pan, 2015; Shinsuke Niwa et al., 2012; Wang et al., 2016). In *Plasmodium*, PbKIN8B could therefore be involved in several steps of microgametogenesis, such as DNA replication, axoneme assembly, function, and male gamete exflagellation.

Using the rodent model *Plasmodium berghei*, we show that PbKIN8B is associated with the axoneme of the microgamete. Its absence causes striking defects in axonemal structure and leads to failure to infect the mosquito and thus complete the parasite lifecycle.

Results

Kinesins in Plasmodium

To study kinesin motor proteins and to determine their potential role in *Plasmodium* male gametogenesis, we first compiled the known data on the proteins and their encoding genes, using the nomenclature by Wickstead et al. (2010). Nine kinesins were identified in *P. falciparum*, but the

genome of several other *Plasmodium* species (*P. berghei*, *P. chabaudi*, *P. yoelii*, *P. knowlesi*) encodes an additional protein, kinesin-4 (PBANKA_1208200) (Table 1). *P. berghei* possesses orthologues for the kinesins identified in *P. falciparum*, either belonging to known kinesin families or currently unclassified (Table 1). Recent RNAseq studies demonstrated expression of *P. berghei* kinesins in sexual stages (male and female) (Otto et al., 2014; Yeoh, Goodman, Mollard, McFadden, & Ralph, 2017). Three kinesins were found specifically expressed in male gametocytes and gametes by proteomic analysis (Khan et al., 2005; Talman et al., 2014): PbKIN8B, KIN13 and KIN15. As KIN13 and KIN15 are essential in the erythrocytic stage, we focussed on PbKIN8B. In *P. berghei*, PbKIN8B is composed of 1460 aa with a predicted molecular weight of 168,81 kDa and encoded by the PB_0202700 gene (4819 nt). PbKIN8B encompasses a classical motor domain positioned centrally [aa 779- 1118] with 8 predicted ATP binding sites [aa 787, 872, 875, 877, 878, 879, 880, 1018] and 3 predicted microtubule interaction sites [aa 1071, 1074, 1077]. With the exception of the kinesin motor domain and of coiled-coil motives in the C-terminal region, no additional protein signatures or nuclear localisation signals (NLS) were detected.

PbKIN8B is specific to male gametocytes and gametes and is associated with the axoneme

According to the classification of kinesins, based on the position of the motor domain within the protein, the central position of the motor domain of PbKIN8B would most likely correspond to a kinesin involved in mitosis (Miki, Okada, & Hirokawa, 2005) and therefore localised in the nucleus. To test this hypothesis, PbKIN8B localization was determined in the rodent model *Plasmodium berghei* by tagging the *Pbkin8B* with *gfp* at the C-terminal end. After transfection, a single crossover recombination at the endogenous PBANKA_0202700 locus resulted in a cell line expressing a *Pbkin8B-gfp* fusion protein. Two independent clones (*Pbkin8B-gfp*-cl4 and *Pbkin8B-gfp*-cl6) were isolated and the correct integration in the genome was confirmed by PCR (Fig S1 A, B).

The expression of the hybrid protein did not impact on the progression of the parasite life cycle. *Pbkin8B-gfp* parasites produced gametocytes in similar quantities to wt parasites with a similar sex

ratio (Fig S1C,D). The parasites were transmitted to mosquitos and naïve mice, similar to wt (see below). The *Pbkin8B-gfp* cell lines express a protein of approximately 180 kDa, recognized by an anti-GFP antibody, consistent with the calculated molecular weight of the tagged protein (*i.e* 187 kDa) (Fig 1A). The hybrid protein is expressed only in the sexual stage and is not detected in asexual parasites or in wt (Fig 1A).

We then studied the cellular localization of PbKIN8B, by following the expression of *Pbkin8B-gfp* by IFA at different stages of the life cycle (Fig 1B). Male and female gametocytes can be easily distinguished during the course of gametogenesis as α–tubulin II and DAPI intensities increase in male gametocytes, while they remain almost constant in female gametocytes. PbKIN8B could not be detected in asexual parasites, nor in female gametocytes. Upon activation by XA, when male gametogenesis is induced *in vitro,* the localization of the *Pbkin8B-gfp* signal changes. The protein first shows a uniform cytosolic distribution in male gametocytes, with the exclusion of the nuclear region which following activation then redistributes as punctiform lines with spatial and temporal dynamics similar to the axonemal marker α–tubulin II (Fig 1B). After exflagellation, the *Pbkin8B-gfp* signal is detected in the male gametes, but it is not seen after fertilization in ookinetes (data not shown). This could be due to a diffuse localization of the protein in the ookinete and the oocyst, hindering its detection under the conditions used for IFA or an absence of PbKIN8B at these stages. The axoneme survives for approximately 5 mins after fertilization, before being depolymerized in the zygote, prior to the formation of the young (retort) ookinete.

PbKIN8B plays a crucial role in exflagellation and fertilization *in vitro*

The axonemal localisation of PbKIN8B and the absence of nuclear staining indicates that it is probably not involved in DNA replication. Several potential roles for PbKIN8B in male gametogenesis could be envisaged: it could be involved in flagellum assembly/functioning and/or exflagellation. We generated *P. berghei* PbKIN8B knock-out parasites (named *ΔPbkin8B*) by double homologous recombination using the PlasmoGem construct PbGEM-267699 replacing the PbKIN8B

encoding gene by a human *dhfr/ts* cassette (Fig S2 A-C). After selection by pyrimethanime and cloning by limiting dilution, two independent *ΔPbkin8B* clones (*ΔPbkin8B* - cl3600 and *ΔPbkin8B* - cl3716) were obtained. Both cell lines show gametocyte numbers and sex ratio similar to wt parasites (Fig S2 D,E).

The *ΔPbkin8B* mutant parasites are able to form asexual and sexual blood stages are formed, therefore mitosis in these stages is normal. Merozoite and ookinete motility appears normal, indicating that the motility of the subpellicular cytoskeleton is functional. The defects in the *ΔPbkin8B* mutant parasites are therefore restricted to microgametogenesis.

In blood containing wt gametocytes, induction by XA leads to the release of male gametes from microgametocytes and their adherence to surrounding red blood cells forming "exflagellation centres". The capacity of *ΔPbkin8B* microgametocytes to exflagellate in response to stimulation by XA *in vitro* was determined in comparison to wt parasites. In *ΔPbkin8B* parasites no exflagellation centres were observed in 10 experiments (5 per clone), even after a prolonged induction period (30 min instead of 15 min). This contrasts strikingly with exflagellation in wt parasites (33,46 ± 17,87 exflagellation centres per 100 male gametocytes, at 15 mpa) (Fig 2A). No free male gametes were observed under these conditions of analysis in the mutant lines. Recognising that rare gametes could have been missed in the mutant even with careful observation and an isolated male gamete could be sufficient to fertilise a female gamete, we performed an *in vitro* ookinete conversion assay to quantify the proportion of activated female gametes that converted into ookinetes. In wt parasites, the mean ookinete conversion rate was 63.5 ± 3.6, whereas it was only of 1.2 ± 1.4 and 0.2± 0.2 for *ΔPbkin8B* clones 3600 and 3716 (Fig 2B), indicating that a few viable male gametes were produced in the mutant able to fertilize the female gametes.

PbKIN8B is essential for the completion of the life cycle *in vivo*

In vitro experiments do not necessarily reflect the complexity of the parasite life cycle, therefore we analysed the life cycle *in vivo* by transmitting wt and mutant parasites to mosquitoes and naïve mice.

We analysed the capacity for infection of *ΔPbkin8B* (2 independent clones), wt and *Pbkin8B-gfp* parasites. Mice were infected with the different parasite lines, *A. stephensi* mosquitoes were allowed to feed on the infected mice.

Eight and twelve days post feeding, the midgut of the mosquitoes was dissected and the number of oocysts per midgut was determined (2 independent experiments). The two *ΔPbkin8B* mutant cell lines produced very few oocysts (mean range of 1.68/1.36 and 1.4/0.76 respectively) in comparison to wt and *Pbkin8B-gfp* parasites, where numerous oocysts were formed (mean values of the 2 replicates of 180/171 and 187/160 oocysts per midgut respectively) (Fig 2C, Table S2). No sporozoites could be detected in the *ΔPbkin8B* oocysts under microscopy.

Since as few as 10 sporozoites would be sufficient to complete the life cycle (Churcher et al., 2017), we tested the ability of the parasites to infect mice. *A. stephensi* mosquitoes fed 21 days prior on mice infected with *ΔPbkin8B*, wt or *Pbkin8B-gfp* parasites were allowed to bite naïve mice. Wt and *Pbkin8B-gfp* fed mosquitoes were able to transmit parasites to the naive mice, as observed on Giemsa stained blood smears at day 5 post feeding. In contrast, mosquitoes fed with *ΔPbkin8B*-cl3600 and cl3716 were unable to transmit parasites to naive mice. Parasitaemia was followed up to 14 days after feeding in the mice bitten by mosquitoes with *ΔPbKIN8B* parasites, but no parasites were seen (Fig 2D).

Dissection of the role of PbKIN8B in male gametogenesis

The *ΔPbkin8B* mutant displays little evidence of of microgametes and is unable to complete the parasite life cycle, indicating a major defect in male gametogenesis. As this process is composed of different events such as host cell egress, DNA replication and axoneme formation, and finally exflagellation, we investigated each of these steps in the *ΔPbkin8B* mutant at different times post activation.

First, we followed cell egress in *ΔPbkin8B* mutant cells and wt cells, using an anti-spectrin antibody, which recognizes the most abundant protein in the red blood cell membrane skeleton. After induction

by XA, both *ΔPbkin8B* and wt gametocytes were able to escape from the host cell membrane as shown by the weaker signal with the anti-spectrin antibody (Fig S3).

Second, we looked at the 3 rounds of endomitoses that occur consecutively during microgametogenesis resulting in a DNA content of 8C. We analysed DNA content in at least 30000 gametocytes at 0, 8 and 15 mpa by XA, using flow cytometry (Fig 3A-C). We compared *ΔPbkin8B* gametocytes to wt and *Δcdpk4* gametocytes, a mutant unable to undergo DNA replication. Gating was established within the YOYO+ population, which was determined by comparison with the negative controls (data not shown). P1 corresponded to the complete YOYO1+ population. At time 0 min, in all cell lines, most gametocytes (male and female) possess a nuclear content of 1C corresponding to the P2 population. Only a few cells with DNA content >1C were detected in wt and *ΔPbkin8B* cells. During the course of the induction, the P2 population decreases slightly in these cell lines, while the P3 population (highest DNA content cells) increases, indicating that the *ΔPbkin8B* microgametocytes replicate their DNA similarly to wt, both in quantity and time frame (Fig 3B, C). The proportion of cells with highest DNA content in the sample (ratio P3/P1) increases by a factor of approximately 3 in wt and 4 in *ΔPbkin8B*. As expected, no change in DNA profile is observed in *Δcdpk4* cells over the time of the experiment (Fig 3C).

Third, we analysed axoneme formation by IFA using an anti α-tubulin II antibody, combined with DAPI staining (Fig 4). From the beginning of activation to 8 mpa, *ΔPbkin8B* and wt gametocytes were indistinguishable by DAPI staining: the DNA positive area became enlarged and the intensity of the signal increased, suggesting that nuclear DNA was replicated in *ΔPbkin8B* parasites similar to wt cells, corroborating the FACS results (Fig 3). At the same time, microtubules were assembled in the cytoplasm, coiled around the enlarged nucleus, though the signal in *ΔPbkin8B* cells looked less intense than in wt cells (Fig 4). At 15 mpa, the replicated DNA separated into 3-8 ‘clumps’ in wt and mutant. At this moment, the overall cell shape differed between mutant and wt parasites. *ΔPbkin8B* microgametocytes remained rounded. Short thin protrusions, which are labelled with the anti α-

tubulin II antibody, could be seen in some of these cells (Fig 4), but they did not separate from the microgametocyte even after 30 mpa. By contrast, at 15 and 30 mpa, exflagellating gametes could be observed in the wt.

PbKIN8B is therefore involved most likely in axoneme assembly/stabilisation and/or exflagellation (axoneme motility), and not in mitosis, as could have been hypothesized on the basis of the position of the motor domain in the protein structure.

PbKIN8B is essential for axoneme assembly in *Plasmodium*

Absence of PbKIN8B disrupts the life cycle of *Plasmodium*, causes defects in microgametogenesis. To better understand the phenotype observed by light microscopy, we examined the ultrastructure of male gametocytes by transmission electron microscopy in wt and mutant cells at 15 and 30 mpa.

At 15 mpa, the gametocytes from wt and *ΔPbkin8B* have egressed from the RBC and were observed at various stages of microgametogenesis (Fig 5a-j). The earlier stages of both wt (Fig 5a, g) and mutant (Fig 5b, h) are characterized by a large spherical central nucleus with dispersed chromatin. When the cytoplasm was examined the wt had a number of developing axonemes predominantly with classical 9 doublet microtubules around 2 central microtubules (Fig 5a, c, d, and Table S3). The microtubules of the axonemes develop from an electron dense basal body and elongate round the periphery of the microgametocyte (Fig 5a, g, i). However, even in wt there were numerous examples of free doublet microtubules and incomplete axoneme formation (S3 Table). In contrast, in the mutant, no complete “9+2” axonemes were observed but doublet and single microtubules were frequently present in the cytoplasm. In cross section, they were randomly distributed (Fig 5e, f) but still appeared to elongate round the periphery of the gametocyte (Fig 5b, h). It was sometimes possible to identify two single microtubules similarly arranged to the central tubules of the axonemes but little evidence of spatial organization of the doublet microtubules around them (Fig 5f). A very few images showed an almost complete circular arrangement, surrounding 1 or 2 singlet microtubules. Identification of radial spokes, connecting outer doublet microtubules to the central pair complex,

was difficult. The microtubules in both wt and mutant appear to grow from electron dense structures (previously identified as basal bodies) (Fig 5b, h).

As the microgametocytes develop (undergo genome replication), multiple nuclear poles were observed in both the wt and mutant (Fig 5i, h). The organization of nuclear poles was similar in both wt and *ΔPbkin8B* consisting of an electron dense cone-like structure from which spindle microtubules radiate with attached kinetochores (insets in Fig 5g, h).

In the later stages of microgametogenesis, in both the wt and *ΔPbkin8B* there was similar chromatin condensation within the nucleus prior to exflagellation (Fig 6a, b). However, while it was possible to observe exflagellation with a flagellum and associated nucleus protruding from the microgametocyte (Fig 6c) and free microgametes in the wt (Fig 6e, f), no free microgametes were observed in the *ΔPbkin8B* samples although very rare examples of cytoplasmic protrusions were identified (Fig. 6d), which contained disorganized doublet microtubules (Fig 6g).

In summary, PbKIN8B does not play a role in genome replication and intranuclear subdivision in gametogenesis, but it is essential for assembly of structured “9+2” axonemes in the cytoplasm. In the absence of viable/motile microgametes, parasites are unable to successfully complete their life cycle.

Discussion

Kinesins are motor proteins, playing important roles in eukaryotes. *P. berghei* possesses members of the kinesin families 4, 5, 8, 13, 15 and 20, as well as three kinesins which could not be associated to known families (Wickstead, Gull, et al., 2010). There is no ortholog of kinesin-4 family member PBANKA_1208200 in *P. falciparum*, even though it is functional and important for growth in the asexual stages in *P. berghei* (Bushell et al., 2017). The restricted number of kinesin encoding genes does not necessarily mean that *Plasmodium* needs these proteins less than other organisms. Malarial kinesins could have multiple roles as it has been shown in other organisms (Dawson et al., 2007; Wickstead, Carrington, Gluenz, & Gull, 2010).

For *Plasmodium*, very little data can be found. According to two transcriptomic studies, all kinesin encoding genes in *P. berghei* are expressed during the sexual stage (Otto et al., 2014; Yeoh et al., 2017). Proteomic studies identified 3 kinesins specific to male gametogenesis (kinesin-8B, -13 and -15) (C. H. S. Garcia et al., 2018; Khan et al., 2005; Talman et al., 2014), but no functional studies have been conducted until now. In other eukaryotes, orthologues for kinesin-4, -5, -8B, -13 and -15 are known to be involved in microtubule dynamics and particularly mitosis and cilia/flagella length regulation (Almeida & Maiato, 2018; Hu et al., 2015; Ma, Wang, & Yang, 2017; Muhia et al., 2016; S. Niwa, 2015; Shinsuke Niwa et al., 2012; Shrestha, Hazelbaker, Yount, & Walczak, 2018; Singh, Pandey, Al-Bassam, & Gheber, 2018; van Riel et al., 2017). Unfortunately, concerning PBANKA_0622400, PBANKA_0609500, PBANKA_0809500, PBANKA_0902400 and PBANKA_1224100, no functional data are available and the number of species possessing orthologues of these proteins is currently very limited, making it difficult to construct any hypothesis concerning their roles.

In other eukaryotes, kinesin-8 family members, which share a family-specific helical neck region (Miki et al., 2005), have been shown to be involved in both mitosis and microtubule regulation in cilia/flagella. The members of the kinesin-8A subfamily are found in different organisms and their roles in mitosis, often promoting microtubule catastrophe, have been studied extensively (Dave et al., 2018; Edzuka & Goshima, 2019; Gergely et al., 2016; Grissom et al., 2009; Messin & Millar, 2014; Savoian & Glover, 2010; Su et al., 2013). In fission yeast, additional roles involving cell polarity and control of cortical microtubule length have been shown (Meadows et al., 2018; West, Malmstrom, Troxell, & McIntosh, 2001). Members of kinesin-8B subfamily have been less studied. They are restricted to ciliated/flagellated organisms (Wickstead, Gull, et al., 2010), but absent in *Drosophila*, *Trypanosoma* or *Chlamydomonas*, inferring a specific role for these proteins in some organisms. The functional information arises from the mammalian orthologue, KIF19A, localized at the ciliary tip. HsKIF19A plays a role in controlling microtubule length in cilia and its absence entails the formation

of abnormally long cilia, causing hydrocephaly and female infertility in mice (Shinsuke Niwa et al., 2012).

Plasmodium possesses 2 members of the kinesin-8 family: PbKIN8B and KIN8X (PBANKA_0805900, belonging to neither the KIN8A nor the KIN8B subfamily). There is currently no information about KIN8X.

PbKIN8B displays its motor domain in a central position, which corresponds to mitotic, non-motile kinesins, such as kinesin-13 proteins (Miki et al., 2005). In this case, a nuclear localization of the protein, as well as defects in DNA replication in its absence, might be expected. In *Plasmodium*, as opposed to metazoan eukaryotes, the nuclear envelope never breaks down. Cytoplasmic kinesins therefore never get access to the spindle during mitosis and nuclear vs. cytoplasmic location is critical. A nuclear localisation signal could not be detected in the PbKIN8B sequence. This complements to the IFA data showing that PbKIN8B is excluded from the nucleus. Moreover, in absence of PbKIN8B DNA replication and spindle activity occur normally in both microgametes and asexual bloodstage parasites. A mitotic role of PbKIN8B during other life stages where mitosis also occurs, such as sporozoite formation and/or liver-stage development, whilst not anticipated, cannot be completely excluded. Unfortunately, no data are available on the expression of PbKIN8B in these stages.

Looking at the different steps in male gametogenesis, we have shown that mutant *ΔPbkin8B* microgametocytes are able to egress from the red blood cell, a step which is independent from DNA replication and axoneme motility (Tewari et al., 2005). Absence of PbKIN8B causes defects in axonemal assembly, accompanied by the presence of singlet and doublet microtubules in the cytoplasm, without complete “9+2” axonemes. *In vivo*, PbKIN8B is essential for completion of the parasite life cycle. Several hypotheses for the role of PbKIN8B can be envisaged.

1) The absence of PbKIN8B could cause defects at the level of the basal body, at the very beginning of the construction of the axoneme. Reduced number of basal bodies have been reported in a different *Plasmodium* mutant (*Δsas-6* (Marques et al., 2015)). SAS-6 is a protein essential for the assembly of

centrioles/basal bodies in many organisms (Gonczy & Hatzopoulos, 2019; Guichard, Hamel, & Gonczy, 2018). While the localisation of SAS-6 is restricted to the basal body end of the axoneme, which becomes the distal tip of the emerged microgamete, PbKIN8B is present along the complete length of the axoneme. We cannot exclude that PbKIN8B is also present at the basal body. In most organisms, basal bodies are composed of triplet microtubules (A, B and C). At the transition zone, microtubules C stop, while microtubules A and B elongate, forming the outside doublet microtubules. The central pair is assembled *de novo* on the transition plate (Dean, Moreira-Leite, & Gull, 2019). In *Plasmodium*, the basal body is composed of only 9 singlet microtubules A (Sinden et al., 1976). To form the doublet microtubules of the axoneme, microtubules B have to be added to the existing microtubules A. It has been recently shown *in vitro* that, under certain conditions, B-microtubules can nucleate on A-microtubules, resulting in a doublet microtubules even in absence of a basal body (Schmidt-Cernohorska et al., 2019). Thus, in *Plasmodium*, where all necessary proteins are present in the cytoplasm and ready for assembly (Sinden, 2015), singlet and doublet microtubules could potentially assemble without a functional basal body.

2) Assuming the basal body in the knockout mutant is functional and able to sustain the elongation of axonemal microtubules, the problem could lie in the stability of the assembled axoneme. As the axoneme grows, the abnormalities due to the absence of PbKIN8B cause the disruption of the connections between elements leading to a fatal dislocation of the structure. Several factors could exacerbate the instability:

First, microtubule sliding, which occurs during axonemal bending. This is caused by coordinated activity of axonemal dyneins, located on the doublet microtubules (for a recent review (Viswanadha, Sale, & Porter, 2017)). In some organisms, like trypanosomes, new and growing flagella start beating very soon after their assembly. This movement could disrupt weakened connections and cause the breakdown of the structure. In *Plasmodium*, fully formed axonemes start beating only seconds before exflagellation, limiting the effect of microtubule sliding on the stability of the structure (Sinden & Croll, 1975).

Second, in most eukaryotes, axonemes are built on cellular protrusions and encased in a membrane. This sheath which in other organisms could stabilize the axoneme is absent in *Plasmodium* due to its intracytoplasmic mode of assembly.

Third, looking at the axoneme in *Plasmodium*, it is obvious that the organism operates with a reduced set of proteins for assembly and functioning. This rudimentary structure, while fast to assemble in the cytoplasm, may be more susceptible to dislocation when just one component is missing. A potential problem could lie at the level of the radial spokes which are difficult to see in the mutant. Complete or partial absence of radial spokes could also cause a fragile structure.

How could PbKIN8B be responsible for the observed phenotype? We propose that PbKIN8B is either directly or indirectly involved in axonemal assembly and stability.

If PbKIN8B is a structural component of the axoneme, its absence could lead directly to structural vulnerability. In *Chlamydomonas reinhardtii*, absence of the kinesin KLP1 leads to defects in motility and loss of two structures associated with the central pair microtubules C2 (Yokoyama, O'Toole, Ghosh, & Mitchell, 2004).

On the other hand, PbKIN8B could play an indirect role and interact with various partners. The identification of putative partners of PbKIN8B is difficult, as PbKIN8B is not conserved in the most commonly used model organisms. Moreover, only few proteins involved in *Plasmodium* male gametogenesis have been identified.

KIN8B could transport elements necessary for assembly or stabilization of the structure. Even with a motor domain in a central position as observed in PbKIN8B, we cannot exclude the possibility that PbKIN8B is motile. We were not able to determine motility along microtubules, as it is difficult to follow gametogenesis in living cells using gfp-tagged proteins.

Even if PbKIN8B is not motile itself, it could associate with other motor proteins. In *Saccharomyces pombe*, the active kinesin-8 is a heterodimeric complex formed by KLP5 and KLP6 (M. A. Garcia, Koonrugsa, & Toda, 2002; Unsworth, Masuda, Dhut, & Toda, 2008; West, Malmstrom, & McIntosh,

2002). PbKIN8B in *P. berghei* displays several coiled-coil motifs adjacent to the motor domain, which could be involved in oligomerization. Taking into account both expression in male gametocytes (this work, (Khan et al., 2005)) and putative NLS signature, kinesin-13 and -15 would be the most likely partners, if PbKIN8B functions as dimer. Interestingly, the search tool STRING (Search Tool for the Retrieval of Interacting Genes/Proteins) (Szklarczyk et al., 2015) proposes several motor proteins (dyneins and kinesins) among potential interactors for PbKIN8B.

Another possibility for an indirect role of PbKIN8B is an interaction with one or several axonemal proteins. In *Plasmodium*, two mutants presenting aberrant axonemes have been reported: *Δsas-6*, mentioned above (Marques et al., 2015) and *Δpf16* (Straschil et al., 2010). As the phenotype observed in *ΔPbkin8B* resembles strongly the one of *Δsas-6*, this protein – or another basal body protein – could be a possible partner of the kinesin. While the localization of PbKIN8B is similar to PbPF16, a protein whose absence causes mainly defects at the level of the central pair, the phenotype of *ΔPbkin8B* is more pronounced. One could imagine that PbKIN8B interacts not only with PbPF16, but at the same time with a second partner, causing cumulative defects. Other potential partners could be proteins belonging to the radial spoke or the nexin-dynein regulatory complexes. If PbKIN8B interacts with a protein essential for the cohesion of the complex, its absence could destabilize the complex, as mentioned above. Finally, it is possible that PbKIN8B interacts with proteins at different locations and/or moments during assembly, once again cumulating destabilizing effects.

The lack of information on molecular actors involved in gametogenesis coupled to a complex and original system of axoneme assembly and gamete production, renders the attribution of partners to PbKIN8B complicated and future studies are necessary to dissect this crucial step in the parasite life cycle.

We have presented the first characterization of kinesin 8B (PbKIN8B) involved in male gametogenesis in *Plasmodium berghei*. This study illustrates the importance of molecular motors in *Plasmodium* and shows that the absence of this kinesin causes severe defects that impede completion of the life cycle. Taken together, our results not only illustrate a previously unknown role for

PbKIN8B in male gametogenesis, but also provide new insights into flagellar organization and function in *Plasmodium*.

Experimental procedures

Ethics statement

All animal work was carried out in accordance with the European regulations and in compliance with the French guidelines and regulations. The project was approved by the Ethic Committee CUVIER (authorization n°68-007).

Generation of transgenic parasites

A pyrimethamine-sensitive clone of *P. berghei* NK65 strain (kindly provided by R. Ménard, Pasteur Institute, France) was used throughout this study to infect mice as described by Janse and collaborators (de Koning-Ward et al., 2000). *P. berghei* was maintained by cyclic passage in 4 to 6 weeks old female Swiss OF1 (Janvier labs, France). The *Pbkin8B-gfp* plasmid was generated by amplifying the final portion of the PbKIN8B coding sequence [nt1978-nt4378] with primers 111 and 112b (S1 Table). A unique restriction site for SacII in the middle of this region was used for single digestion and single crossover (vertical bar Fig S1A). The construct was inserted into the vector pl0016 (MRA-785 (BEI Resources)). The stop codon was removed and the gfp coding sequence was fused in-frame to the coding sequence. The plasmid also contained the *T. gondii* dhfr/ts resistance marker conveying resistance to pyrimethamine (Franke-Fayard MBP 2004). For PbKIN8B replacement (*ΔPbkin8B* lines), the transfection vector was sourced from the Sanger Institute (PbGEM-267699) (Schwach et al., 2015) and linearized by NotI prior to transfection. Details on tagging and knockout of PBANKA_020270 production are shown in Figs S1 and S2. Transfections were performed as described previously (Janse et al., 2006). Following drug selection, independent clonal populations of each genetic background were selected by limiting dilution and subsequent

genotyping. Transfection experiments for gene disruption and gene tagging strategies were done in duplicate on different days using different batches of material.

Genotypic analysis of mutants

The genotypes of *Pbkin8B-gfp* and *ΔPbkin8B* parasites were analysed by PCR with specific primers (Figs S1 and S2, Table S1). Briefly, for the C-terminal fusion *Pbkin8B-gfp* tagged parasites, integration was verified using primer 109 upstream of the amplified region and primer 115 in the *Pbkin8B-gfp* construct. Primers 53 and 54 served to confirm the presence of the resistance cassette. For the gene knockout parasites, two diagnostic PCR reactions were used as shown in Fig S2. Amplification by primers GT and GW2 was used to determine successful integration of the selectable marker at the targeted locus whereas primers QCR1 and QCR2 were used to verify deletion of the gene (S1 Table).

Gametocyte preparation, exflagellation assays and ookinete conversion rates

Preparation of *P. berghei* gametocytes was realized as described previously (Beetsma et al., 1998). Briefly, mice were injected intraperitoneally with 0.1 ml of 25 mg/l phenylhydrazine (to induce hyper-reticulocytosis) two days prior to infection by 10^7 parasites. To reduce asexual parasitaemia, mice received sulfadiazine (10 mg/L) in their drinking water from day 5 to 7 after infection. On day seven, gametocyte-infected blood was collected for direct exflagellation assays or gametocyte purification before immunofluorescence assays, electron microscopy experiments or cytometry measurements as described by Billker *et al.* (2004). After collection of whole blood on heparin, white blood cells were removed on CF11 cellulose (Whatman) columns. Gametocytes were separated from uninfected erythrocytes on a Nycodenz cushion made up from 48% Nycodenz stock (27.6% w/v Nycodenz in 5.0 mM Tris-HCl pH 7.2, 3.0 mM KCl, 0.3 mM EDTA) and RPMI1640 medium containing 25 mM HEPES (Sigma), 5% FCS, 4 mM sodium bicarbonate, pH 7.3. Gametocytes were harvested from the interface and washed three times in the appropriate buffer for the subsequent

protocol. All manipulations were carried out at 19–22°C. Mature male and female gametocytes can be differentiated by gametocyte pigmentation following Giemsa staining (males appear blue and females pink).

For exflagellation assays, blood was diluted in 10 volumes of exflagellation medium (100 µM xanthurenic acid (XA) (Sigma) in RPMI 1640 (Thermo Fisher Scientific), pH 7.4). The actively moving gametes interacting with neighbouring RBC (exflagellation centres) were recorded 20 minutes post activation (mpa) by phase contrast microscopy in 10 x 1mm^2 Malassez squares using a 40× objective. The number of exflagellation centres was then expressed relative to 100 male gametocytes for each sample. To perform the ookinete conversion assay, blood was first mixed at a 1:1 ratio in ookinete medium (RPMI pH8, 10% foetal calf serum, 100 µM XA). After 24 h to allow completion of gametogenesis and fertilization, ookinete conversion assays were performed as previously described (Tewari et al., 2005) by incubating samples with monoclonal antibody 13.1 (antibody against Pb28), conjugated with Cy3. The conversion rate corresponds to the proportion of ookinetes to all 13.1-positive cells (unfertilized macrogametes and ookinetes). Experiments were realized in biological triplicate.

Western blotting

Asexual stages and gametocytes were isolated as described above. After the addition of Laemmli sample buffer, the samples were boiled and equal quantities of total protein were loaded on a 7 % SDS-polyacrylamide gel, before transfer to a nitrocellulose membrane (Thermo Fisher). Western blot analysis of *Pbkin8B-gfp* was performed under reducing conditions, using an anti-gfp rabbit antibody (1/3000, Abcam) coupled to an alkaline phosphatase conjugated goat anti-rabbit globulin (1/5000, Thermo Fisher).

Mosquito infection

For mosquito infections, 3- to 8-day-old female adult *A. stephensi* mosquitoes were raised as previously described (Dimopoulos et al., 1998). Day 3 post mouse-infection, mosquitoes were allowed to feed on anaesthetized infected mice for 20 min (Rodriguez et al., 2002; Sinden et al., 2002), mosquitoes which had not fed, were discarded.

Engorged mosquitoes were dissected at day 8 or day 12 post feeding and the number of oocysts counted. For bite-back experiments, mosquitoes were infected with wild type or *ΔPbkin8B* parasites and after 21 days mice were infected by the bite of these mosquitoes. After 5 days parasitaemia was determined on mouse blood by blood smears and Giemsa staining and was followed for 14 days for mice infected by *ΔPbkin8B* parasites. All experiments were realized in duplicate. Differences between groups were calculated with Fisher's exact test for prevalence, Mann-Whitney test for intensity.

Indirect immunofluorescence assay (IFA)

Purified gametocytes were fixed at different time points in 3.7% (v/v) formaldehyde overnight at 4°C and processed as described previously (Becker et al., 2010). After a brief wash in PBS, cells were allowed to adhere onto poly-L-lysine coated slides and were then permeabilized by 0.5% (v/v) NP40 in PBS for 15 min. After a 30 minute saturation step, slides were incubated for 2 h with the first antisera (diluted 1/1000 for rabbit anti α–tubulin II, 1/2000 for rabbit anti-GFP, 1/200 for rabbit anti-spectrin, non-diluted for mouse TAT1 (Woods et al., 1989) followed by three washes before incubation for 1 h with appropriate fluorescently labelled secondary antibodies (Alexa Fluor®488 goat anti-mouse IgG (H+L), Alexa Fluor® 568 goat anti-rabbit IgG (H+L) both diluted 1/300 (Invitrogen)). After a 5 min DAPI incubation (5 microgram/ml), followed by a final wash, slides were mounted in Vectashield (Vector Laboratories). Parasites were visualized on a Nikon Eclipse TE 300 DV inverted microscope with a 100x oil objective mounted on a piezo electric device using appropriate fluorescence emission filters. Image acquisition (z-series) was performed with a back

illuminated cooled detector (Photometrics CoolSnap HQ, 12 bit, RoperScientific, France) using a 0.20 µm step. Image processing was performed using Image J software (http://rsb.info.nih.gov/ij/).

Electron microscopy

Gametocyte samples (described above) were fixed 15 and 30 mpa in 2.5% glutaraldehyde in 0.1 M phosphate buffer and processed for electron microscopy as previously described (Ferguson et al., 2005). Briefly, samples were post fixed in 1% osmium tetroxide, treated en bloc with 2 % uranyl acetate, dehydrated and embedded in epoxy resin. Thin sections were stained with uranyl acetate and lead citrate prior to examination in a JEOL1200EX electron microscope (Jeol UK Ltd).

Flow cytometry

To measure nuclear DNA content of activated gametocytes (wt, *ΔPbkin8B* and *Δcdpk4* - a mutant viable in blood infection that does not undergo DNA replication during microgametogenesis (Billker et al., 2004)) by flow cytometry, purified gametocytes were transferred into ookinete culture medium for activation of gamete formation. At 0, 8 and 15 mpa, cells were fixed overnight at 4°C in 0.04% glutaraldehyde. Blood of naïve mice was fixed in the same conditions and used as a negative control. DNA was stained with YOYO-1 (Bouillon et al., 2013). Briefly, gametocytes and blood samples were treated for 10 minutes with 0.25% TritonX100 in PBS after centrifugation at 100g for 5 minutes. They were then treated with 0.05 mg/ml RNase A/T1 (Thermo Scientific™) for 4 h at 37°C. Finally, DNA was stained with 10.24 µM YOYO-1 (Invitrogen™). A gametocyte sample was duplicated for an unstained control. After overnight incubation at 4°C, the supernatant was replaced by FACSFlow solution and flow cytometry data acquired on a FACSVerse (BD Biosciences). Data processing and analysis were performed using the FACSuite Software v 1.0.5 (BD Biosciences). YOYO-1 fluorescence was excited with a blue laser (20 mW) at 488 nm and the signal was detected at 527 +/- 16 nm. Quality control based on FSC-A vs SSC-A and FSC-H vs FSC-A gating was applied to remove debris and doublets respectively. Then, histograms of YOYO-1-A signal (in log scale) were

analysed to determine nucleic acid content. Gates were established resulting in populations P1 corresponding to the complete YOYO+ population, P2 composed of cells with the lowest DNA content (1C), and P3, corresponding to cells with the highest DNA content. For each sample the FACS profile was established and the ratio of populations (P2 and P3) was expressed as a percentage of P1.

Figure Legends

Fig 1. *Pbkin8B-gfp* is specifically expressed in male gametocytes and localizes to the axoneme.

(A) Western blot of *Pbkin8B-gfp* erythrocytic stages showing expression of a 190 kDa protein only in gametocytes (*Pbkin8B-gfp* gam). No signal was detected in *Pbkin8B-gfp* asexual stages (*Pbkin8B-gfp* asex) nor in wt gametocytes (wt gam). Similar results were obtained with both clones.

(B) Immunofluorescence assay of *Pbkin8B-gfp* male and female gametocytes at 8 minutes post activation (mpa) and exflagellating male gametes at 15 mpa. DAPI staining of DNA is seen in blue, anti-α tubulin II in red and anti-gfp in green. Immunofluorescence images correspond to the maximum intensity projection of the z-series. Gfp images were treated post capture using ImageJ for better visualisation (increase by 2 times for gfp gametocytes and 10 times for exflagellating microgametes). The colocalisation of α tubulin II and gfp evidence male specific expression of *Pbkin8B-gfp*. Scale bar: 2 µm.

Fig 2. *ΔPbkin8B* parasites are unable to complete the parasite life cycle

(A, B) *In vitro* analysis of the *ΔPbkin8B* mutant. (A) Comparison of exflagellation rates between *ΔPbkin8B* (clones 3600 and 3716) and wt cells at 15 mpa. Numbers of exflagellation centres are expressed relatively to 100 microgametocytes. (B) Comparison of ookinete conversion rates between *ΔPbkin8B* (clones 3600 and 3716) and wt. For each replicate (n=5), the conversion rate was calculated as the percentage of macrogametes that developed into ookinetes. Values represent an average of more than 800 cells. SD are reported as bars on the figures. Asterisk (*) indicate statistically significant differences with p-values lower than 0,0001.

(C, D) *In vivo* analysis of the *ΔPbkin8B* mutant (2 clones). (C) Comparison of mosquito infection rates between *ΔPbkin8B* (clones 3600 and 3716), *Pbkin8B-gfp* and wt parasites. At day 8 and day 12 post feeding, infected *A. stephensi* mosquitoes were dissected and oocysts, were counted in each

midgut. Detailed results are presented in Supplemental table 2. (D) Analysis of transmission of *ΔPbkin8B, Pbkin8B-gfp* and wt parasites from mosquitoes to naïve mice. *A. stephensi* mosquitoes infected respectively with *ΔPbkin8B, Pbkin8B-gfp* and wt parasites, were allowed to bite naïve mice. Infection of mice was monitored at day 5 and day 12 on Giemsa stained blood smears.

Fig 3. *ΔPbkin8B* cells are able to replicate their DNA during male gametogenesis

(A) Time course analysis of gametocyte DNA by flow cytometry. Purified mixed gametocytes from *ΔPbkin8B, Δcdpk4* (unable to undergo DNA replication) and wt parasites were fixed at times 0, 8 and 15 mpa and DNA was labelled with YOYO-1. Gates were established defining populations P1 (total YOYO+ population), P2 (1N DNA content cells), and P3 (multinucleated cells).

(B, C) Evolution over time of populations P2 and P3. Proportion of P2 cells (B), respectively P3 cells (C), relative to YOYO+ cells at times 0, 8 and 15 mpa.

Fig 4. *ΔPbkin8B* parasites are able to replicate DNA and produce microtubules, but cannot release male gametes.

Immunofluorescence assay of wt and *ΔPbkin8B* male gametocytes from beginning of activation to 30 mpa. DAPI staining of DNA is seen in blue and anti-α tubulin II in red. Immunofluorescence images correspond to the maximum intensity projection of the z-series. During the course of activation, wt microgametocytes increased nuclear content and formed microgametes. *ΔPbKIN8B* microgametocytes also replicated DNA and assembled microtubules in the cytoplasm. However, they were not able to release microgametes. Scale bar: 2 µm.

Fig 5. *ΔPbkin8B* microgametocytes display a modified ultrastructure with disorganised axonemes.

Electron micrographs of various developmental stages of microgametogenesis in wt and *ΔPbkin8B* parasites at 15 and 30 mpa. Bars represent 1µm in a, d, g, i, k, m and 100 nm in all other micrographs.

a. Low power through a wt microgametocyte showing the central nucleus (N) with a number of axonemes (A) running round the peripheral cytoplasm. b. Low power through a *ΔPbkin8B* microgametocyte showing the large central nucleus (N) with longitudinally running microtubules (Mt). c. Detail of the cytoplasm of wt microgametocyte illustrating cross section through two axonemes (A). d. Enlargement of an axoneme showing the 9+2 arrangement of the microtubules. e. Detail of the cytoplasm of a *ΔPbkin8B* gametocyte showing a cross section through s number of randomly distributed microtubules mostly as doublets (Mt). f. Enlargement of a group of microtubules showing two single microtubules (arrowheads) with randomly distributed doublet microtubules (arrows). g. Low power of a mid-stage wt microgametocyte showing the central nucleus (N) with a number of nuclear poles (NP). Insert. Detail of a nuclear pole (NP) and radiating microtubules with attached kinetochore (K). h. Low power of a mid-stage *ΔPbkin8B* gametocyte showing the central nucleus (N) and associated nuclear pole (NP). Insert. Detail of a nuclear pole (NP) and radiating microtubules with attached kinetochore (K). i. Detail from the cytoplasm of a wt parasite from the enclosed area g showing a longitudinal section through the basal body (BB) and axoneme (A).

j. Detail from cytoplasm of a *ΔPbkin8B* gametocyte from the enclosed area in b showing longitudinally running microtubule (Mt) emanating from an electron dense structure possible basal body (BB).

Fig 6. *ΔPbkin8B* microgametocytes condenses chromatin but do not release male gametes.

Electron micrographs of late developmental stages of microgametogenesis in wt and *ΔPbkin8B* parasites at 15 and 30 mins. Bars represent 1µm in a, b, c and d and 100 nm in all other micrographs. a. Low power of a late stage wt microgametocyte showing the nucleus (N) with peripherally condensed heterochomatin (Ch). b. Low power of a late *ΔPbkin8B* gametocyte showing the nucleus with condensed chromatin (Ch). c. Low power of a late microgametocyte undergoing exflagellation with the flagellum (F) and associated nucleus (N) protruding from the surface. d. Low power of a late *ΔPbkin8B* gametocyte showing a centrally located nucleus (N) with condensed chromatin (Ch) and a

cytoplasmic process from the surface containing microtubules (Mt). e. Longitudinal section through a free microgamete showing the relationship between the nucleus (N) and the flagellum (F). f. Cross section through a free wt microgamete illustrating the electron dense nucleus (N) and associated flagellum (F). g. Detail of a cross section through a cytoplasmic process from a *ΔPbkin8B* gametocyte showing disorganized duplet microtubules (Mt).

Acknowledgements

We wish to thank Joy Alonso and Nathalie Dogna for animal care, Elisabeth Mouray for technical help and Philippe Bastin (Institut Pasteur, Paris) for critical reading of the manuscript and helpful discussions.

This project was funded by ATM from Muséum National d'Histoire Naturelle, Paris.

REFERENCES

Almeida, A. C., & Maiato, H. (2018). Chromokinesins. *Curr Biol, 28*(19), R1131-R1135. doi:10.1016/j.cub.2018.07.017

Becker, C. A., Malandrin, L., Depoix, D., Larcher, T., David, P. H., Chauvin, A., . . . Bonnet, S. (2010). Identification of three CCp genes in Babesia divergens: novel markers for sexual stages parasites. *Mol Biochem Parasitol, 174*(1), 36-43. doi:10.1016/j.molbiopara.2010.06.011

Beetsma, A. L., van de Wiel, T. J., Sauerwein, R. W., & Eling, W. M. (1998). Plasmodium berghei ANKA: purification of large numbers of infectious gametocytes. *Exp Parasitol, 88*(1), 69-72. doi:10.1006/expr.1998.4203

Bennink, S., Kiesow, M. J., & Pradel, G. (2016). The development of malaria parasites in the mosquito midgut. *Cell Microbiol, 18*(7), 905-918. doi:10.1111/cmi.12604

Billker, O., Dechamps, S., Tewari, R., Wenig, G., Franke-Fayard, B., & Brinkmann, V. (2004). Calcium and a calcium-dependent protein kinase regulate gamete formation and mosquito transmission in a malaria parasite. *Cell, 117*(4), 503-514.

Billker, O., Lindo, V., Panico, M., Etienne, A. E., Paxton, T., Dell, A., . . . Morris, H. R. (1998). Identification of xanthurenic acid as the putative inducer of malaria development in the mosquito. *Nature, 392*(6673), 289-292. doi:10.1038/32667

Bouillon, A., Gorgette, O., Mercereau-Puijalon, O., & Barale, J. C. (2013). Screening and evaluation of inhibitors of Plasmodium falciparum merozoite egress and invasion using cytometry. *Methods Mol Biol, 923*, 523-534. doi:10.1007/978-1-62703-026-7_36

Bushell, E., Gomes, A. R., Sanderson, T., Anar, B., Girling, G., Herd, C., . . . Billker, O. (2017). Functional Profiling of a Plasmodium Genome Reveals an Abundance of Essential Genes. *Cell, 170*(2), 260-272 e268. doi:10.1016/j.cell.2017.06.030

Churcher, T. S., Sinden, R. E., Edwards, N. J., Poulton, I. D., Rampling, T. W., Brock, P. M., . . . Blagborough, A. M. (2017). Probability of Transmission of Malaria from Mosquito to Human Is Regulated by Mosquito Parasite Density in Naive and Vaccinated Hosts. *PLoS Pathog, 13*(1), e1006108. doi:10.1371/journal.ppat.1006108

Dave, S., Anderson, S. J., Sinha Roy, P., Nsamba, E. T., Bunning, A. R., Fukuda, Y., & Gupta, M. L., Jr. (2018). Discrete regions of the kinesin-8 Kip3 tail differentially mediate astral microtubule stability and spindle disassembly. *Mol Biol Cell, 29*(15), 1866-1877. doi:10.1091/mbc.E18-03-0199

Dawson, S. C., Sagolla, M. S., Mancuso, J. J., Woessner, D. J., House, S. A., Fritz-Laylin, L., & Cande, W. Z. (2007). Kinesin-13 regulates flagellar, interphase, and mitotic microtubule dynamics in Giardia intestinalis. *Eukaryot Cell, 6*(12), 2354-2364. doi:10.1128/EC.00128-07

de Koning-Ward, T. F., Fidock, D. A., Thathy, V., Menard, R., van Spaendonk, R. M., Waters, A. P., & Janse, C. J. (2000). The selectable marker human dihydrofolate reductase enables sequential genetic manipulation of the Plasmodium berghei genome. *Mol Biochem Parasitol, 106*(2), 199-212.

Dean, S., Moreira-Leite, F., & Gull, K. (2019). Basalin is an evolutionarily unconstrained protein revealed via a conserved role in flagellum basal plate function. *Elife, 8*. doi:10.7554/eLife.42282

Dimopoulos, G., Seeley, D., Wolf, A., & Kafatos, F. C. (1998). Malaria infection of the mosquito Anopheles gambiae activates immune-responsive genes during critical transition stages of the parasite life cycle. *EMBO J, 17*(21), 6115-6123. doi:10.1093/emboj/17.21.6115

Edzuka, T., & Goshima, G. (2019). Drosophila kinesin-8 stabilizes the kinetochore-microtubule interaction. *J Cell Biol, 218*(2), 474-488. doi:10.1083/jcb.201807077

Ferguson, D. J., Henriquez, F. L., Kirisits, M. J., Muench, S. P., Prigge, S. T., Rice, D. W., . . . McLeod, R. L. (2005). Maternal inheritance and stage-specific variation of the apicoplast in Toxoplasma gondii during development in the intermediate and definitive host. *Eukaryot Cell, 4*(4), 814-826. doi:10.1128/EC.4.4.814-826.2005

Filarsky, M., Fraschka, S. A., Niederwieser, I., Brancucci, N. M. B., Carrington, E., Carrio, E., . . . Voss, T. S. (2018). GDV1 induces sexual commitment of malaria parasites by antagonizing HP1-dependent gene silencing. *Science, 359*(6381), 1259-1263. doi:10.1126/science.aan6042

Francia, M. E., Dubremetz, J. F., & Morrissette, N. S. (2015). Basal body structure and composition in the apicomplexans Toxoplasma and Plasmodium. *Cilia, 5*, 3. doi:10.1186/s13630-016-0025-5

Franke-Fayard, B., Trueman, H., Ramesar, J., Mendoza, J., van der Keur, M., van der Linden, R., . . . Janse, C. J. (2004). A Plasmodium berghei reference line that constitutively expresses GFP at a high level

throughout the complete life cycle. *Mol Biochem Parasitol, 137*(1), 23-33. doi:10.1016/j.molbiopara.2004.04.007

Garcia, C. H. S., Depoix, D., Queiroz, R. M. L., Souza, J. M. F., Fontes, W., de Sousa, M. V., . . . Charneau, S. (2018). Dynamic molecular events associated to Plasmodium berghei gametogenesis through proteomic approach. *J Proteomics, 180*, 88-98. doi:10.1016/j.jprot.2017.11.009

Garcia, M. A., Koonrugsa, N., & Toda, T. (2002). Two kinesin-like Kin I family proteins in fission yeast regulate the establishment of metaphase and the onset of anaphase A. *Curr Biol, 12*(8), 610-621.

Gergely, Z. R., Crapo, A., Hough, L. E., McIntosh, J. R., & Betterton, M. D. (2016). Kinesin-8 effects on mitotic microtubule dynamics contribute to spindle function in fission yeast. *Mol Biol Cell, 27*(22), 3490-3514. doi:10.1091/mbc.E15-07-0505

Gonczy, P., & Hatzopoulos, G. N. (2019). Centriole assembly at a glance. *J Cell Sci, 132*(4). doi:10.1242/jcs.228833

Grissom, P. M., Fiedler, T., Grishchuk, E. L., Nicastro, D., West, R. R., & McIntosh, J. R. (2009). Kinesin-8 from fission yeast: a heterodimeric, plus-end-directed motor that can couple microtubule depolymerization to cargo movement. *Mol Biol Cell, 20*(3), 963-972. doi:10.1091/mbc.E08-09-0979

Guichard, P., Hamel, V., & Gonczy, P. (2018). The Rise of the Cartwheel: Seeding the Centriole Organelle. *Bioessays, 40*(4), e1700241. doi:10.1002/bies.201700241

Gupta, M. L., Jr., Carvalho, P., Roof, D. M., & Pellman, D. (2006). Plus end-specific depolymerase activity of Kip3, a kinesin-8 protein, explains its role in positioning the yeast mitotic spindle. *Nat Cell Biol, 8*(9), 913-923. doi:10.1038/ncb1457

Hu, Z., Liang, Y., Meng, D., Wang, L., & Pan, J. (2015). Microtubule-depolymerizing kinesins in the regulation of assembly, disassembly, and length of cilia and flagella. *Int Rev Cell Mol Biol, 317*, 241-265. doi:10.1016/bs.ircmb.2015.01.008

Ishikawa, T. (2017). Axoneme Structure from Motile Cilia. *Cold Spring Harb Perspect Biol, 9*(1). doi:10.1101/cshperspect.a028076

Janse, C. J., Ramesar, J., & Waters, A. P. (2006). High-efficiency transfection and drug selection of genetically transformed blood stages of the rodent malaria parasite Plasmodium berghei. *Nat Protoc, 1*(1), 346-356. doi:10.1038/nprot.2006.53

Kafsack, B. F., Rovira-Graells, N., Clark, T. G., Bancells, C., Crowley, V. M., Campino, S. G., . . . Llinas, M. (2014). A transcriptional switch underlies commitment to sexual development in malaria parasites. *Nature, 507*(7491), 248-252. doi:10.1038/nature12920

Kent, R. S., Modrzynska, K. K., Cameron, R., Philip, N., Billker, O., & Waters, A. P. (2018). Inducible developmental reprogramming redefines commitment to sexual development in the malaria parasite Plasmodium berghei. *Nat Microbiol, 3*(11), 1206-1213. doi:10.1038/s41564-018-0223-6

Khan, S. M., Franke-Fayard, B., Mair, G. R., Lasonder, E., Janse, C. J., Mann, M., & Waters, A. P. (2005). Proteome analysis of separated male and female gametocytes reveals novel sex-specific Plasmodium biology. *Cell, 121*(5), 675-687. doi:10.1016/j.cell.2005.03.027

Kosugi, S., Hasebe, M., Tomita, M., & Yanagawa, H. (2009). Systematic identification of cell cycle-dependent yeast nucleocytoplasmic shuttling proteins by prediction of composite motifs. *Proc Natl Acad Sci U S A, 106*(25), 10171-10176. doi:10.1073/pnas.0900604106

Ma, D. D., Wang, D. H., & Yang, W. X. (2017). Kinesins in spermatogenesis. *Biol Reprod, 96*(2), 267-276. doi:10.1095/biolreprod.116.144113

Marques, S. R., Ramakrishnan, C., Carzaniga, R., Blagborough, A. M., Delves, M. J., Talman, A. M., & Sinden, R. E. (2015). An essential role of the basal body protein SAS-6 in Plasmodium male gamete development and malaria transmission. *Cell Microbiol, 17*(2), 191-206. doi:10.1111/cmi.12355

McHugh, T., Gluszek, A. A., & Welburn, J. P. I. (2018). Microtubule end tethering of a processive kinesin-8 motor Kif18b is required for spindle positioning. *J Cell Biol, 217*(7), 2403-2416. doi:10.1083/jcb.201705209

Meadows, J. C., Messin, L. J., Kamnev, A., Lancaster, T. C., Balasubramanian, M. K., Cross, R. A., & Millar, J. B. (2018). Opposing kinesin complexes queue at plus tips to ensure microtubule catastrophe at cell ends. *EMBO Rep, 19*(11). doi:10.15252/embr.201846196

Messin, L. J., & Millar, J. B. (2014). Role and regulation of kinesin-8 motors through the cell cycle. *Syst Synth Biol, 8*(3), 205-213. doi:10.1007/s11693-014-9140-z

Miki, H., Okada, Y., & Hirokawa, N. (2005). Analysis of the kinesin superfamily: insights into structure and function. *Trends Cell Biol, 15*(9), 467-476. doi:10.1016/j.tcb.2005.07.006

Muhia, M., Thies, E., Labonte, D., Ghiretti, A. E., Gromova, K. V., Xompero, F., . . . Kneussel, M. (2016). The Kinesin KIF21B Regulates Microtubule Dynamics and Is Essential for Neuronal Morphology, Synapse Function, and Learning and Memory. *Cell Rep, 15*(5), 968-977. doi:10.1016/j.celrep.2016.03.086

Niwa, S. (2015). Kinesin superfamily proteins and the regulation of microtubule dynamics in morphogenesis. *Anat Sci Int, 90*(1), 1-6. doi:10.1007/s12565-014-0259-5

Niwa, S., Nakajima, K., Miki, H., Minato, Y., Wang, D., & Hirokawa, N. (2012). KIF19A is a microtubule-depolymerizing kinesin for ciliary length control. *Developmental cell, 23*(6), 1167-1175.

Oda, T., Abe, T., Yanagisawa, H., & Kikkawa, M. (2016). Structure and function of outer dynein arm intermediate and light chain complex. *Mol Biol Cell, 27*(7), 1051-1059. doi:10.1091/mbc.E15-10-0723

Otto, T. D., Bohme, U., Jackson, A. P., Hunt, M., Franke-Fayard, B., Hoeijmakers, W. A., . . . Janse, C. J. (2014). A comprehensive evaluation of rodent malaria parasite genomes and gene expression. *BMC Biol, 12*, 86. doi:10.1186/s12915-014-0086-0

Ouji, M., Augereau, J. M., Paloque, L., & Benoit-Vical, F. (2018). Plasmodium falciparum resistance to artemisinin-based combination therapies: A sword of Damocles in the path toward malaria elimination. *Parasite, 25*, 24. doi:10.1051/parasite/2018021

Prevo, B., Scholey, J. M., & Peterman, E. J. G. (2017). Intraflagellar transport: mechanisms of motor action, cooperation, and cargo delivery. *FEBS J, 284*(18), 2905-2931. doi:10.1111/febs.14068

Roberts, A. J., Kon, T., Knight, P. J., Sutoh, K., & Burgess, S. A. (2013). Functions and mechanics of dynein motor proteins. *Nat Rev Mol Cell Biol, 14*(11), 713-726. doi:10.1038/nrm3667

Rodriguez, M. C., Margos, G., Compton, H., Ku, M., Lanz, H., Rodriguez, M. H., & Sinden, R. E. (2002). Plasmodium berghei: routine production of pure gametocytes, extracellular gametes, zygotes, and ookinetes. *Exp Parasitol, 101*(1), 73-76.

Savoian, M. S., & Glover, D. M. (2010). Drosophila Klp67A binds prophase kinetochores to subsequently regulate congression and spindle length. *J Cell Sci, 123*(Pt 5), 767-776. doi:10.1242/jcs.055905

Schmidt-Cernohorska, M., Zhernov, I., Steib, E., Le Guennec, M., Achek, R., Borgers, S., . . . Guichard, P. (2019). Flagellar microtubule doublet assembly in vitro reveals a regulatory role of tubulin C-terminal tails. *Science, 363*(6424), 285-288. doi:10.1126/science.aav2567

Schwach, F., Bushell, E., Gomes, A. R., Anar, B., Girling, G., Herd, C., . . . Billker, O. (2015). PlasmoGEM, a database supporting a community resource for large-scale experimental genetics in malaria parasites. *Nucleic Acids Res, 43*(Database issue), D1176-1182. doi:10.1093/nar/gku1143

Shrestha, S., Hazelbaker, M., Yount, A. L., & Walczak, C. E. (2018). Emerging Insights into the Function of Kinesin-8 Proteins in Microtubule Length Regulation. *Biomolecules, 9*(1). doi:10.3390/biom9010001

Sigrist, C. J., de Castro, E., Cerutti, L., Cuche, B. A., Hulo, N., Bridge, A., . . . Xenarios, I. (2013). New and continuing developments at PROSITE. *Nucleic Acids Res, 41*(Database issue), D344-347. doi:10.1093/nar/gks1067

Sinden, R. E. (1983). The cell biology of sexual development in plasmodium. *Parasitology, 86 (Pt 4)*, 7-28.

Sinden, R. E. (2015). The cell biology of malaria infection of mosquito: advances and opportunities. *Cell Microbiol, 17*(4), 451-466. doi:10.1111/cmi.12413

Sinden, R. E., Butcher, G. A., & Beetsma, A. L. (2002). Maintenance of the Plasmodium berghei life cycle. *Methods Mol Med, 72*, 25-40. doi:10.1385/1-59259-271-6:25

Sinden, R. E., Canning, E. U., & Spain, B. (1976). Gametogenesis and fertilization in Plasmodium yoelii nigeriensis: a transmission electron microscope study. *Proc R Soc Lond B Biol Sci, 193*(1110), 55-76. doi:10.1098/rspb.1976.0031

Sinden, R. E., & Croll, N. A. (1975). Cytology and kinetics of microgametogenesis and fertilization in Plasmodium yoelii nigeriensis. *Parasitology, 70*(1), 53-65.

Singh, S. K., Pandey, H., Al-Bassam, J., & Gheber, L. (2018). Bidirectional motility of kinesin-5 motor proteins: structural determinants, cumulative functions and physiological roles. *Cell Mol Life Sci, 75*(10), 1757-1771. doi:10.1007/s00018-018-2754-7

Sinha, A., Hughes, K. R., Modrzynska, K. K., Otto, T. D., Pfander, C., Dickens, N. J., . . . Waters, A. P. (2014). A cascade of DNA-binding proteins for sexual commitment and development in Plasmodium. *Nature, 507*(7491), 253-257. doi:10.1038/nature12970

Straschil, U., Talman, A. M., Ferguson, D. J., Bunting, K. A., Xu, Z., Bailes, E., . . . Rita, T. (2010). The Armadillo repeat protein PF16 is essential for flagellar structure and function in Plasmodium male gametes. *PLoS One, 5*(9), e12901. doi:10.1371/journal.pone.0012901

Su, X., Arellano-Santoyo, H., Portran, D., Gaillard, J., Vantard, M., Thery, M., & Pellman, D. (2013). Microtubule-sliding activity of a kinesin-8 promotes spindle assembly and spindle-length control. *Nat Cell Biol, 15*(8), 948-957. doi:10.1038/ncb2801

Szklarczyk, D., Franceschini, A., Wyder, S., Forslund, K., Heller, D., Huerta-Cepas, J., . . . von Mering, C. (2015). STRING v10: protein-protein interaction networks, integrated over the tree of life. *Nucleic Acids Res, 43*(Database issue), D447-452. doi:10.1093/nar/gku1003

Talman, A. M., Prieto, J. H., Marques, S., Ubaida-Mohien, C., Lawniczak, M., Wass, M. N., . . . Sinden, R. E. (2014). Proteomic analysis of the Plasmodium male gamete reveals the key role for glycolysis in flagellar motility. *Malar J, 13*, 315. doi:10.1186/1475-2875-13-315

Tewari, R., Dorin, D., Moon, R., Doerig, C., & Billker, O. (2005). An atypical mitogen-activated protein kinase controls cytokinesis and flagellar motility during male gamete formation in a malaria parasite. *Mol Microbiol, 58*(5), 1253-1263. doi:10.1111/j.1365-2958.2005.04793.x

Unsworth, A., Masuda, H., Dhut, S., & Toda, T. (2008). Fission yeast kinesin-8 Klp5 and Klp6 are interdependent for mitotic nuclear retention and required for proper microtubule dynamics. *Mol Biol Cell, 19*(12), 5104-5115. doi:10.1091/mbc.E08-02-0224

van Riel, W. E., Rai, A., Bianchi, S., Katrukha, E. A., Liu, Q., Heck, A. J., . . . Akhmanova, A. (2017). Kinesin-4 KIF21B is a potent microtubule pausing factor. *Elife, 6*. doi:10.7554/eLife.24746

Viswanadha, R., Sale, W. S., & Porter, M. E. (2017). Ciliary Motility: Regulation of Axonemal Dynein Motors. *Cold Spring Harb Perspect Biol, 9*(8). doi:10.1101/cshperspect.a018325

Wang, D., Nitta, R., Morikawa, M., Yajima, H., Inoue, S., Shigematsu, H., . . . Hirokawa, N. (2016). Motility and microtubule depolymerization mechanisms of the Kinesin-8 motor, KIF19A. *Elife, 5*. doi:10.7554/eLife.18101

West, R. R., Malmstrom, T., & McIntosh, J. R. (2002). Kinesins klp5(+) and klp6(+) are required for normal chromosome movement in mitosis. *J Cell Sci, 115*(Pt 5), 931-940.

West, R. R., Malmstrom, T., Troxell, C. L., & McIntosh, J. R. (2001). Two related kinesins, klp5+ and klp6+, foster microtubule disassembly and are required for meiosis in fission yeast. *Mol Biol Cell, 12*(12), 3919-3932. doi:10.1091/mbc.12.12.3919

Wickstead, B., Carrington, J. T., Gluenz, E., & Gull, K. (2010). The expanded Kinesin-13 repertoire of trypanosomes contains only one mitotic Kinesin indicating multiple extra-nuclear roles. *PLoS One, 5*(11), e15020. doi:10.1371/journal.pone.0015020

Wickstead, B., Gull, K., & Richards, T. A. (2010). Patterns of kinesin evolution reveal a complex ancestral eukaryote with a multifunctional cytoskeleton. *BMC Evol Biol, 10*, 110. doi:10.1186/1471-2148-10-110

Woods, A., Sherwin, T., Sasse, R., MacRae, T. H., Baines, A. J., & Gull, K. (1989). Definition of individual components within the cytoskeleton of Trypanosoma brucei by a library of monoclonal antibodies. *J Cell Sci, 93 (Pt 3)*, 491-500.

Yeoh, L. M., Goodman, C. D., Mollard, V., McFadden, G. I., & Ralph, S. A. (2017). Comparative transcriptomics of female and male gametocytes in Plasmodium berghei and the evolution of sex in alveolates. *BMC Genomics, 18*(1), 734. doi:10.1186/s12864-017-4100-0

Yokoyama, R., O'Toole, E., Ghosh, S., & Mitchell, D. R. (2004). Regulation of flagellar dynein activity by a central pair kinesin. *Proc Natl Acad Sci U S A, 101*(50), 17398-17403. doi:10.1073/pnas.0406817101

Supplementary material

Table S1. Primer sequences for construction of *Pbkin8B-gfp* vector and verification of integration of *Pbkin8B-gfp*, respectively *ΔPbkin8B*, in the *P. berghei* genome

Primer	***kin8B-gfp* construct and diagnostic**
111 (SacII)	TCC *CCGCGG* GGGCCTGACACATCTAATAG
112b (KpnI)	CATG *CCATGG* TTTTATTTTTTATAATGTTAAAAAGATTTGAG
109	GAAGGAACCGAACTATTAAATG
115	CTGGGTATCTCGCAAAGCATTG
124b	CACTTTGATGTTTCGAAACCTG
34	TTTCCCAGTCACGACGTTG

Primer	***ΔPbkin8B* diagnostic**
GW2b	GGGTGACTTTGGTGACAGATACTAC
QCR1	AGCGAGAAGGAATGCCACTACT
QCR2	ACTCTCTTCTCCACATGCGT
GT	GCCCAGGCCCACAAATGTGC

Table S2. Prevalence and Intensity of mosquito infections

Genotype	Prevalence (% infected *A. stephensi* mosquitoes)	Mean intensity (oocysts number/midgut)	Range of oocysts number	N (number of mosquitoes)
wt	96	180,26	0-407	50
Δ*KIN8B-cl3600*	24 *	1,68 *	0-17	50
Δ*KIN8B-cl3716*	18 *	1,4 *	0-16	50
KIN8B-gfp	98	187,02	0-369	50

Genotype	Prevalence (% infected *A. stephensi* mosquitoes)	Mean intensity (oocysts number/midgut)	Range of oocysts number	N (number of mosquitoes)
WT	98	171,74	0-367	50
Δ*KIN8B-cl3600*	20 *	1,36 *	0-12	50
Δ*KIN8B-cl3716*	10 *	0,76 *	0-12	50
KIN8B-gfp	92	160,36	0-391	50

For each replicate, mice with similar parasitaemias were fed to mosquitoes. Fully fed mosquitoes were kept until midgut dissection, midguts were mounted on slides and oocysts were counted under the microscope. Differences between groups were calculated with Fisher's exact test for prevalence, Mann-Whitney test for intensity. Asterisk * indicate statistically significant differences with p-values lower than 0.0001 and 0.005, respectively.

Table S3. Quantification of microtubule structures in *ΔPbkin8B* and wt gametocytes.

	9+2 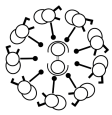	**9+1** 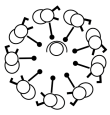	**9+0** 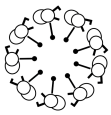	**>6+2** 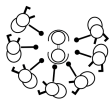	**>6+0**	**3-6** 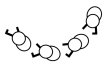	**Doublets** **or**	**Singlets** **or**	**Cell number**
wt	60	6	10	7	2	13	5	0	18
ΔPbkin8B	1			3	4	26	292	113	47

Arrangement of doublet microtubules in circles, with or without a central pair of microtubules, semi-circles or isolated doublet, respectively singlet microtubules, were counted in *ΔPbkin8B* and wt gametocytes.

Fig S1. Generation and genotypic analysis of *Pbkin8B-gfp* parasites.

(A, B) Generation and genotypic analysis of *Pbkin8B-gfp* parasites. (A) Schematic representation of *Pbkin8B* locus before and after insertion of a plasmid containing a partial *Pbkin8B* sequence fused to a gfp tag. Single homologous recombination occurred between the plasmid and the homologous region of the 3'-terminal part of the genomic locus of *Pbkin8B*. Selection was realized using the *Toxoplasma gondii dhfr/ts* resistance marker present in the plasmid. (B) Analysis of genomic DNA from *Pbkin8B-gfp* (clones 4 and 6) and wt parasites by PCR. PCR amplifications were realised to verify integration of the construct in the correct locus using primers detailed in Supplemental Table 2. Lanes 2, 5 and 8 correspond to clone 4; lanes 3, 6 and 9 correspond to clone 6. PCR amplification confirmed correct integration of the construct (lanes 2 and 3), absence of wt genotype (lanes 5 and 6) and of episomal plasmid (lanes 8 and 9).

(C, D) Phenotypic analysis of gametocyte production of *Pbkin8B-gfp* and wt on Giemsa stained blood smears. (C) The number of gametocytes was determined for 4 infected mice per genotype. (D) Male sex ratio of *Pbkin8B-gfp* clones 4 and 6 is similar to wt. Differences between groups were not statistically different. SD are reported as bars on the figures.

Fig S2. Genotypic and phenotypic analysis of *ΔPbkin8B* parasites.

(A-C) Generation and genotypic analysis of *ΔPbkin8B* parasites. (A) Schematic representation of *Pbkin8B* locus before and after replacement of the coding sequence by human dihydrofolate reductase thymidilate synthase / yeast cytosine deaminase and uridyl phosphoribosyl transferase (*hdhfr/yfcu*) gene which confers resistance to pyrimethamine through homologous recombination with the 5′ and 3' homology arms of *Pbkin8B* (PBANKA_020270). Primer positions for verification of replacement are indicated by arrows. (B, C) Analysis of genomic DNA from *ΔPbkin8B* (clones 3600 and 3716) and wt parasites by PCR. (B) PCR amplifications were realised to verify integration of the construct in the correct locus using primer GT and primer GW2. (C) Amplifications with primers QCR2 and QCR1 confirm the absence of *Pbkin8B* gene in the two *ΔPbkin8B* clones.

(D, E) Phenotypic analysis of gametocyte production of *ΔPbkin8B* and wt on Giemsa stained blood smears. (D) The number of gametocytes was determined for 4 infected mice per genotype (i.e wt, *ΔPbkin8B* clone 3600 and clone 3716). (E) Male sex ratio of *ΔPbkin8B* (clones 3600 and 3716) is similar to wt. Differences between groups were not statistically different. SD are reported as bars on the figures.

Fig S3. After activation *ΔPbKIN8B gametocytes* egress quickly from red blood cells

Immunofluorescence assay of wt and *ΔPbkin8B* male gametocytes at 0 and 8 mpa. DAPI staining of DNA is seen in blue, TAT1 in green and anti-spectrin in red. Immunofluorescence images correspond to the maximum intensity projection of the z-series. At 8 mpa, the erythrocyte membrane is degraded compared to 0 mpa, while microtubules have formed in the cytoplasm. Scale bar: 2 µm.

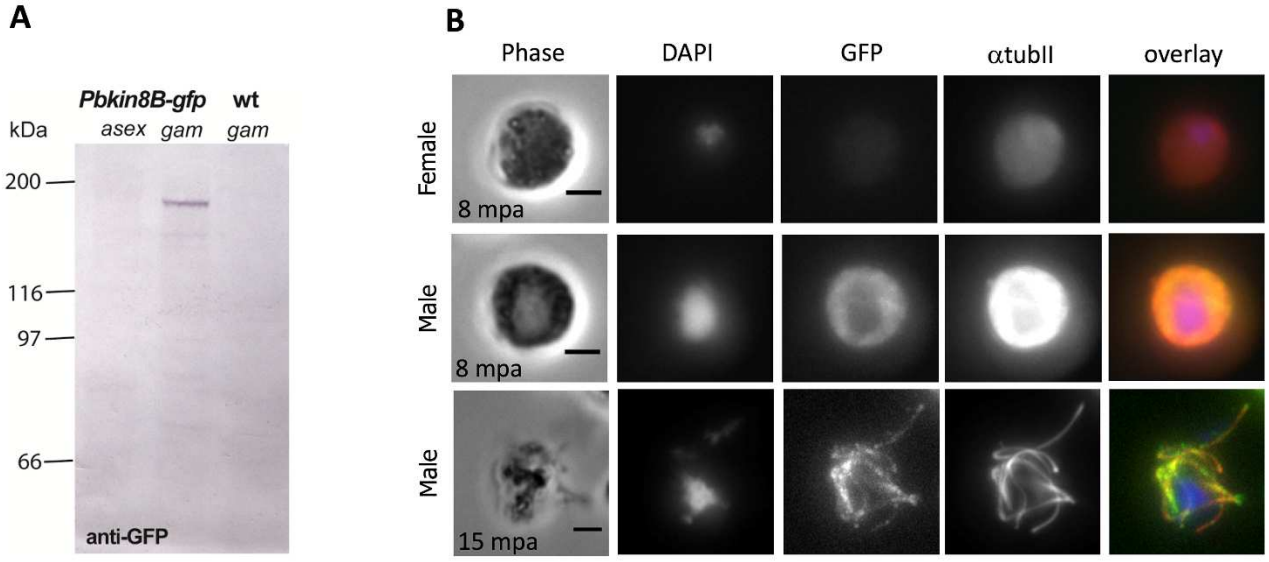

Depoix et al., Figure 1

A

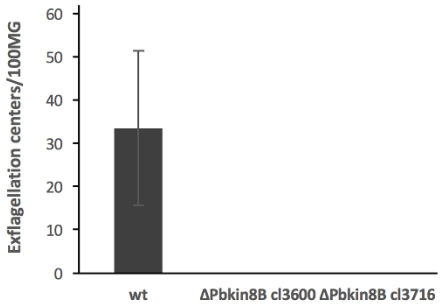

B

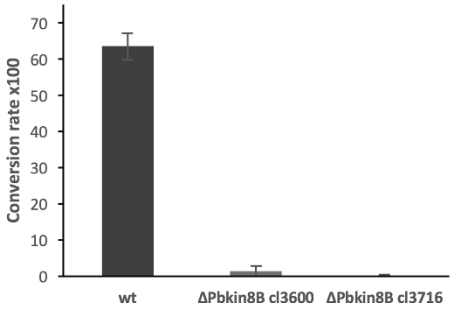

C

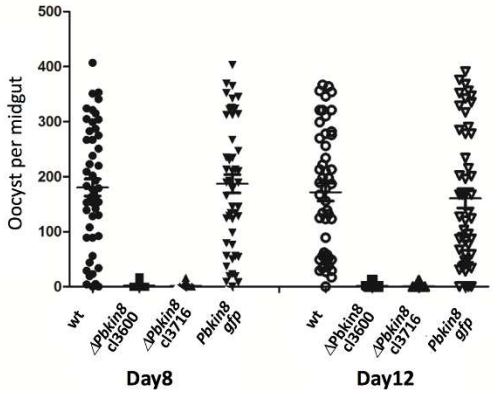

D

Genotype	Number of mosquitoes	Mouse parasitaemia (d5)
wt	43	2/2
ΔPbkin8B-cl3600	38	0/2*
ΔPbkin8B-cl3716	40	0/2*
Pbkin8B-gfp	32	2/2

Depoix et al., Figure 2

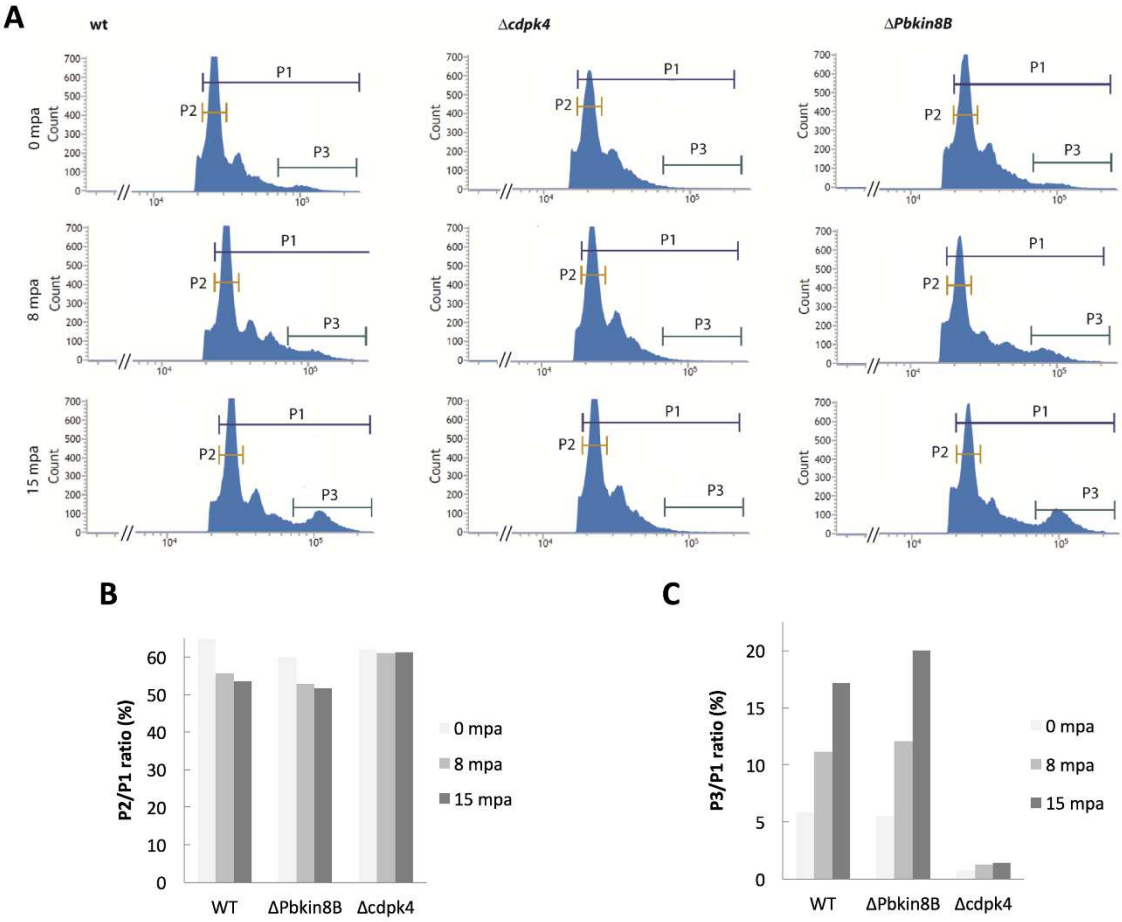

Depoix et al., Figure 3

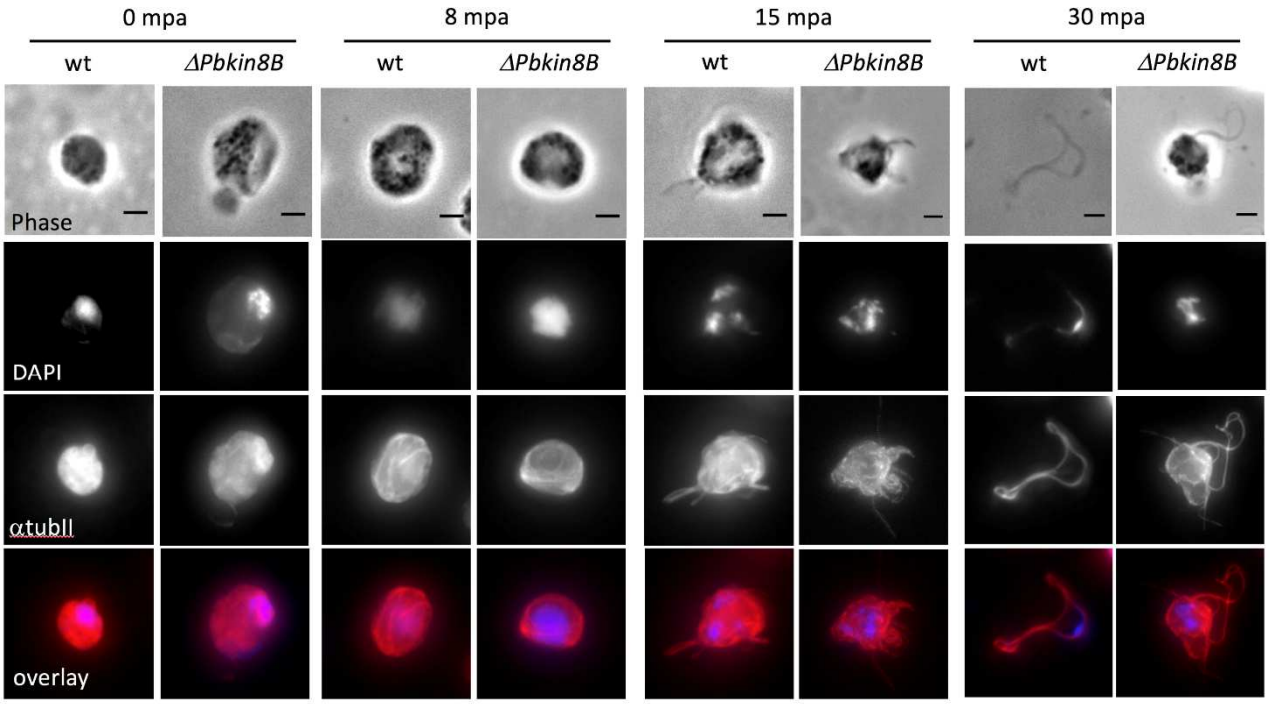

Depoix et al., Figure 4

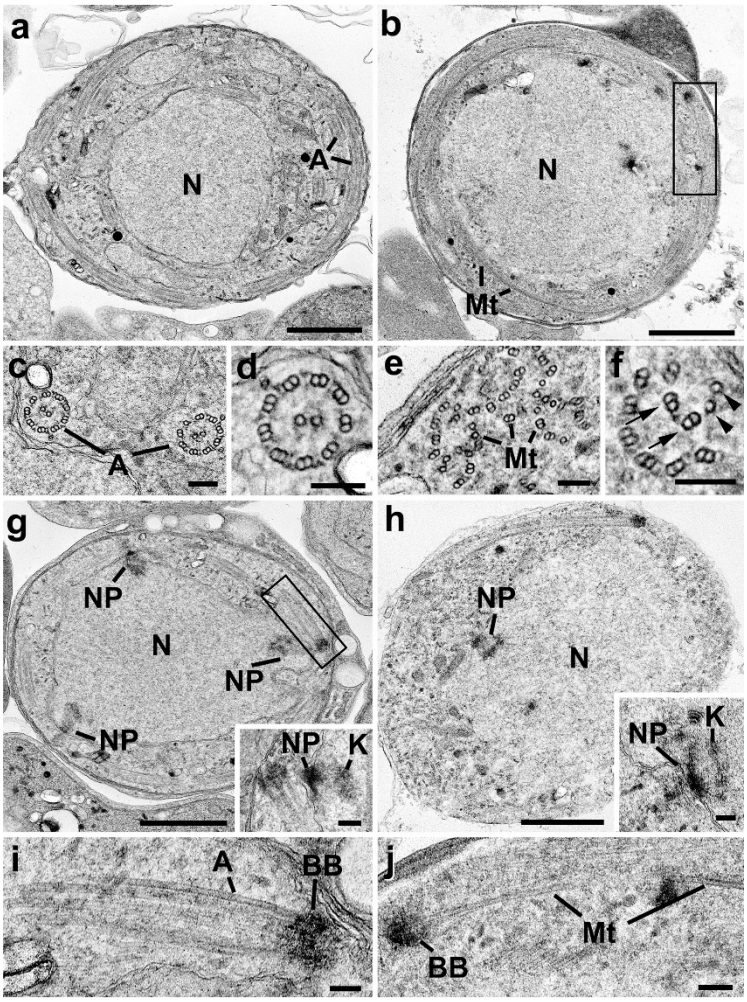

Depoix et al., Figure 5

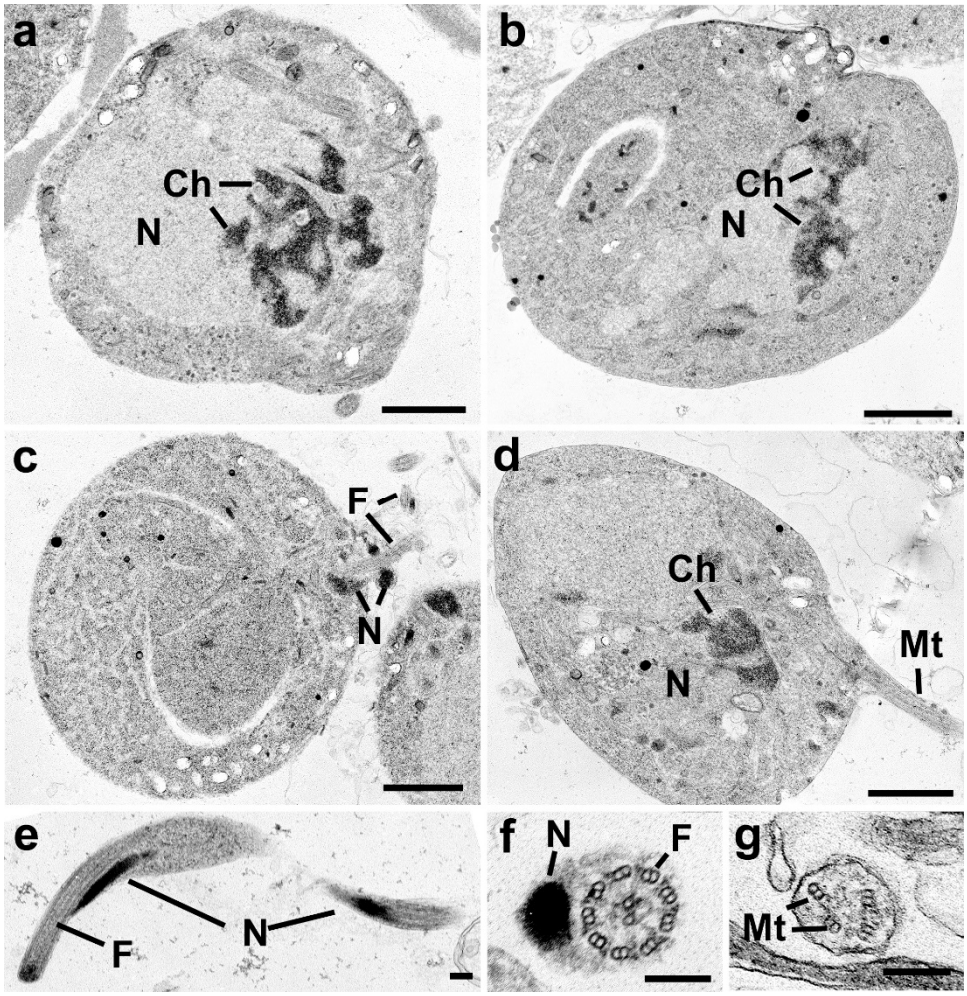

Depoix et al., Figure 6

Table 1: Main characteristics of *Plasmodium berghei* kinesins: protein features, proteomic data in sexual stages, phenotypic analysis in erythrocytic stages

Kinesin family (Pb gene ID/Pf gene ID)	Protein features	Gametocyte	Male gamete	Asexual Phenotype
Kinesin 4 (PBANKA_1208200) – 2876 aa	ATP/Coil WD40 NLS	Female Mixed		slow
Kinesin-5 (PBANKA_0807700/ PF3D7_0317500) – 1440 aa	ATP/MT Coil NLS	ND		ND
Kinesin-8X (PBANKA_0805900/PF3D7_0319400) – 1409 aa	ATP/MT Coil NLS	ND		dispensable
Kinesin-8B (PBANKA_0202700/PF3D7_0111000) – 1460 aa	**ATP/MT**	**Male** **Mixed**	**yes**	**dispensable**
Kinesin-13 (PBANKA_1458300 / PF3D7_1245100) – 1025 aa	ATP/ MT	Female Male Mixed	yes	essential
Kinesin-15 (PBANKA_1458800/PF3D7_1245600) – 1414 aa	ATP	Male Mixed	yes	essential
Kinesin-20* (PBANKA_0622400/PF3D7_0724900) – 2113 aa	ATP/MT Coil NLS	ND		dispensable
Kinesin-X3* (PBANKA_0609500/PF3D7_1211000) – 1603 aa	ATP/MT NLS	Mixed		ND
Kinesin-X4* (PBANKA_0902400/PF3D7_1146700 – 771 aa	ATP Coil	ND		dispensable
Kinesin-like (PBANKA_1224100/PF3D7_0806600) – 727 aa	ATP/Coil NLS	ND		slow

Gene identifiers are shown for *P. berghei* ANKA and *P. falciparum* 3D7 (Plasmodb.org). Seven proteins have been associated to known kinesin families (nomenclature from (Wickstead, Gull, et al., 2010), three proteins could not be classified. Protein features were determined using PROSITE (Sigrist et al., 2013) and cNLS mapper (Kosugi, Hasebe, Tomita, & Yanagawa, 2009). In addition to the conserved kinesin motor domain with ATP binding sites and microtubule interaction (MT) sites, most proteins display coiled-coil motifs, which could be involved in protein oligomerisation. Kinesin-4 presents a WD40 motif, often implicated in protein-protein interactions. Proteomic data of purified male and female gametocytes (Khan et al., 2005), male gametes (Talman et al., 2014), and phenotypic data of asexual stages (Bushell et al., 2017) are presented when available. The asterisk indicate a difference in family affiliation between Plasmodb.org and Wickstead et al (2010) (Wickstead, Gull, et al., 2010). The characteristics of PbKIN8B are highlighted in bold. The motor domain is represented by an orange oval, ATP binding sites are shown in blue and microtubule interacting sites in red. Protein features are depicted by coloured polygons (coil-coil region in blue and WD40 region in green).